TR 66034

FEBRUARY 1966

UNLIMITED

ROYAL AIRCRAFT ESTABLISHMENT

TECHNICAL REPORT No. 66034

THERMAL CONDUCTANCE OF LAP-JOINTS IN VACUUM

by

A. B. Osborn

W. N. Mair

MINISTRY OF AVIATION

FARNBOROUGH HANTS.

U.D.C. No. 536.212.2 : 621.884.052.2 : 533.5 : 669.715

ROYAL AIRCRAFT ESTABLISHMENT

Technical Report No. 66034

February 1966

THERMAL CONDUCTANCE OF LAP-JOINTS IN VACUUM

by

A. B. Osborn

W. N. Mair

SUMMARY

Experiments on the thermal conductance, in vacuum, of lap-jointed specimens of aluminium-clad L72, and unclad L70, aluminium alloys (4% Cu; 0.7% Si; 0.7% Mn) are described. The specimens were strips of thin sheet fastened with rivets, or nuts and bolts. The effects of variability of riveting technique, temperature, thermal cycling, overlap area, bolting-torque, burrs, and interlayers of paint, anti-corrosive jointing compound, indium and electrical insulators were studied. In general, the results support a mechanism of high heat transfer, by metallic conduction, near the rivets or bolts only. This hypothesis is discussed, and it is suggested that the thermal behaviour of the specimens is described better in terms of an additional length of heat-conduction path than by a conventional heat transfer coefficient.

It was found, if burrs are removed, that both careful bolt-tightening and standard, aircraft-construction, riveting techniques produce thermally good lap-joints for which the effect of the doubled thickness is equal to, or greater than, the opposing effect of the interfacial thermal resistance.

Departmental Reference: CPM 60

CONTENTS

1 INTRODUCTION

This paper describes experiments made to obtain data, on the thermal conductance of riveted and bolted joints between metals, that would be relevant to the enginecring design of space-vehicles. The problems of the thermal balance of a space-vehicle are those of spreading, and finally radiating to space, the heat, received from the sun and dissipated by electronic packages, in such a way that no part of the vehicle exceeds, at any time, its maximum operating temperature. Radiation is the best way of transferring heat over large distances; however for small distances conduction can give a useful contribution. A joint in a metallic conduction path introduces a thermal resistance at the interface. At atmospheric pressure, gaseous conduction assists in the transfer of heat between two metals pressed together; in the vacuum of space (see Appendix D), this contribution is absent.

The interfacial resistance of a joint occurs because only the peaks of microscopic surface irregularities make actual contact. If the contact pressure is applied uniformly over the joint area, there is, for most flat engineering surfaces, a fairly uniform distribution of contact points; the number increases with surface smoothness. An increase in the pressure causes deformation and flow of the contacting asperities, which increase both in size and number until the area of real contact is sufficient to support the load. The area of real contact is[1] usually only a small fraction of the total area of the interface (see Section 5). Since the thermal conductance of the metals is usually greater than that of any fluid filling the gap, the lines of heat flow converge towards the contact points where they are restricted to narrow channels thus causing[2] a "constriction resistance". Several analyses of the idealized situation have been published[3,4,5], and experimental results show[6,7,8,9,10,11] that the thermal conductance of an interface varies as predicted with thermal conductivity, mechanical pressure, surface hardness and surface finish. Guarded hot plate thermal conductivity apparatus, in which the pressure is applied uniformly over the area of the interface, was used and the results given in terms of the coefficient of heat transfer h, i.e., the heat flux per unit temperature difference across the interface.

However, such results are not directly applicable to the types of joints actually made by engineers. In normal aircraft practice, joints are fastened by rivets or bolts, and the contact pressure is no longer uniform over the interface. The pressure is high under the head of the fastener[12],

but is negligible elsewhere. Consideration of the transmission of load through elastic layers by isolated fasteners shows[13] that the pressure decreases with distance from the centre-line of the bolt or rivet, and at small distances[14] (of the order of one diameter) falls to zero and is replaced by a "tension". This implies that it is only the regions under the heads of the bolts or rivets that are in good physical contact, and hence provide good thermal conductance, and suggests that the use of excessive closing pressure may tend to distort the metal sheets and produce a worsening of the contact for regions of overlap away from the fasteners. In addition, the fastener itself provides an additional heat-conduction path. Thus, most of the heat transfer takes place close to the fasteners and the concept of a uniform heat transfer coefficient is invalid. In this paper, the results are presented in terms of an additional length $\Delta\ell$, defined in Section 3, to be added to the conduction path to allow for interfacial resistance. A relation between $\Delta\ell$ and h, for uniform interfaces, is derived in Appendix C.

The results reported here are for experiments on lap-jointed aluminium alloy sheets, fastened with either rivets or nuts and bolts. The effect of the inherent variability of riveting on the thermal conductance was studied using specimens with overset or underset rivets - outside the normal acceptance limits of the aircraft industry (see Appendix A). Other factors examined included the effects of bolting torque, temperature and temperature cycling, overlap area and the use of multiple rows of fasteners, burrs, surface cladding with pure aluminium, and interlayers of indium , paint and anti-corrosive jointing compound.

The broad conclusions is that thermally good ($\Delta\ell \sim 0$) lap-joints can be made readily, provided that reasonable care is taken of sheet surfaces, that burrs are removed carefully, that bolts are tightened properly and that rivets are set using standard aircraft-construction techniques to pass standard visual inspection.

In addition, a few experiments are described for electrically insulated joints of possible application to the insulated connection to heat sinks of, for example, transistors.

2 EXPERIMENTAL METHOD

2.1 Specimens

Most of the specimens were made from L72, aluminium alloy, sheet - the structural material of the U.K.3 satellite. This sheet is clad, on both sides, with pure aluminium of thickness 5% that of the sheet. The core alloy is

aluminium containing 4% copper, 0.7% silicon and 0.7% manganese. L72 material is heat-treated in its final form, and aged at room temperature. This leaves the surface layer of pure aluminium in an annealed condition, which should be ideal for making good thermal contact; to check this, a few specimens were made from L70 sheet, which is the same core alloy in unclad form.

Each specimen was made by lap-jointing two rectangular strips of sheet material: the joints were fastened either by $\frac{1}{8}$" diameter SP80 rivets* (size 404) or by 6BA stainless steel nuts and bolts (or screws); burrs, raised in drilling clearance holes for the fasteners, were carefully removed before the strips were assembled. The rivets were closed by machine, at various settings, or by hand using a pneumatic gun (see Appendix A). Nuts and bolts were tightened using torque spanners.

The various types of specimen and the patterns of fasteners used are illustrated in Fig.1. The overall length of each specimen was about 25 cm. For the earlier experiments, most of the specimens were made to a pattern A, 3 cm wide, thickness of order 1 mm (20 swg for L72, 0.002" Al cladding; 18 swg for L70) and with an overlap of 2.5 cm: pattern B was used to obtain an increased heat flux. In later experiments, the standard riveting patterns C, D and E were used.

Thermocouples were used to measure the distribution of temperature along each specimen. Short lengths of chromel and alumel wires were spot-welded to the specimens (see Appendix B); thermocouple location was accurate to about $\pm\frac{1}{4}$ mm. Throughout the experiments there was a gradual improvement in thermocouple technique; this is discussed in Appendices B and D.

2.2 Test apparatus

In essence, the apparatus consisted of two copper blocks against which the ends of a specimen were clamped (see Fig.2). The clamping plates were of copper, 5/16" thick, backed by $\frac{1}{4}$" plates of mild steel. The upper block, containing a nichrome heater, was supported by stainless steel brackets from the lower, water-cooled block. (The lower block also contained a heating element; its use is described in Appendix D). Boron nitride washers were used to reduce heat losses to these brackets. Thermally insulating supports were used between the lower block and the brass base-plate of the vacuum apparatus.

---

* Al, 2% Cu alloy (L86), which does not age-harden appreciably.

A large glass bell-jar covered the apparatus and was evacuated through a hole in the base-plate, by a 4" oil-diffusion pump. Two vacuum-tight sockets carried the thermocouple leads through the base-plate to a selector switch outside the vacuum system. These sockets were 24 way Plessey Mark IV sockets, specially sealed with "Glyptal" cement and O-ring gaskets.

2.3 Experimental procedure

Six lap-jointed specimens, with short thermocouple wires already attached were clamped in position between the two copper blocks. The thermocouple wires were then electrically welded to similar wires from the base-plate sockets. The apparatus was covered by the bell-jar and evacuated to a final pressure of about 5×10^{-5} torr.

Water-cooling was then applied to the lower block, and the upper block was heated rapidly to the desired temperature. The heater current was then reduced to a predetermined value, allowing the specimens to reach a steady state temperature distribution in about $1\frac{1}{2}$ hours. Temperature observations were observed repeatedly, at about hourly intervals, to check that the steady state had been reached.

The normal conditions of test were a hot block temperatue of about $100^{\circ}C$ and a water-cooled cold block temperatue of about $20^{\circ}C$. Occasionally a hot block temperature of about $200^{\circ}C$ was used; attention is drawn to these "hot" experiments in the results of Section 4.

The thermocouple emf's, between the hot junctions on the specimens and a reference junction held at $0^{\circ}C$ in melting ice, were measured by a digital voltmeter to an accuracy of ± 10 μV, i.e. a temperature accuracy of about $\pm\frac{1}{4}^{\circ}C$. The $\frac{1}{4}$ mm uncertainty in hot-junction location is equivalent to an additional temperature uncertainty of about $1/10^{\circ}C$.

The magnitude of the heat losses from the sides of a specimen, due to conduction in the residual gas in the apparatus and to radiation, is discussed in Appendix D. It is shown to be negligible in a vacuum of 5×10^{-5} torr for a surface emissivity of 10% of a "black-body" or less.

3 THEORY OF THE METHOD

In the experiments described in Section 2, specimens of lap-jointed strips conduct heat from a hot block to a cold sink. For thin strips of high thermal conductivity k, the flow of heat, in the absence of radiation and

gas-conduction losses, is essentially one-dimensional. In the steady state, the temperature gradient $\partial T/\partial x$ along the strip and the heat flow Q are constant everywhere apart from the overlap region ($-a/2 \leq x \leq a/2$ - Fig.3); and

$$Q = -k u v \frac{\partial T}{\partial x} \tag{1}$$

where u is the width and v the thickness of the strips.

The specimen temperature is normally observed at three positions; two thermocouples are attached symmetrically with respect to the lap-joint ($x = \mp\frac{1}{2}b$) and a third to the colder strip at $x = c + \frac{1}{2}b$. If the observed temperatures, in the steady state, are θ_1, θ_2 and θ_3 respectively,

$$\frac{\partial T}{\partial x} = \frac{\theta_3 - \theta_2}{c} \tag{2}$$

is the temperature gradient away from the joint itself, and the temperature drop ΔT across the lap-joint - i.e., the difference in temperature of the hotter strip at $x = -\frac{1}{2}a$ and the colder strip at $x = \frac{1}{2}a$ - is given by

$$\Delta T = (\theta_1 - \theta_2) + (b - a) \frac{\partial T}{\partial x} . \tag{3}$$

Division by $-\partial T/\partial x$ gives the length ℓ_o of a simple strip, of the same section uv, of the same material having the same ΔT for the same heat flow Q. Therefore, as regards its thermal resistance, a lap-joint, with an actual length a of overlap, can be described as having an "effective length" ℓ_o of continuous, unjointed, strip. Hence,

$$\ell_o = c\left(\frac{\theta_1 - \theta_2}{\theta_2 - \theta_3}\right) - (b - a) . \tag{4}$$

Thus a strip of total length ℓ, with an overlap length a, behaves thermally as a continuous strip of length $\ell + (\ell_o - a)$. The additional length $\Delta\ell$, due to the thermal resistance of the joint, is given by

$$\Delta\ell = \ell_o - a = c\left(\frac{\theta_1 - \theta_2}{\theta_2 - \theta_3}\right) - b . \tag{5}$$

A high value of $\Delta\ell$ indicates a poor thermal contact; for a joint in which the effect of the doubled thickness of the overlap outweighs the interfacial resistance $\Delta\ell$ is negative.

4 RESULTS

In this section, the results are given in terms of the additional length $\Delta\ell$, defined in Section 3; the lower the value of $\Delta\ell$, the better is the thermal contact.

4.1 Riveted L72 lap-joints

4.1.1 Preliminary results for machine-set rivets

In the first experiments, the effects of variability of riveting technique on the thermal conductance of lap-joints was studied. The methods of machine- and hand-riveting used, and the variability produced, are described in Appendix A. The specimens were 3 cm wide strips of 20 swg L72, joined with two rivets (pattern A of Fig.1); the length of overlap was 1". Before riveting, the drilling burrs were carefully removed.

It was noticed that the surface of the strips around the rivets were deformed to produce a saucer-shaped depression; the effect was slight with underset rivets, and greater with overset rivets.

The results obtained with overset and underset machine-riveting are given in Table 1: the first column gives the specimen number - the middle digit indicating the machine setting, 3 for underset and 4 for overset rivets. Subsequent columns give the values of $\Delta\ell$ in millimetres obtained in successive experiments. Between experiments the apparatus was cooled to room temperature and, in some cases, air was let in and pumped out again. In all experiments the cold block was water-cooled at about 20°C: in most experiments the temperature of the hot block was about 100°C; the results, for the three experiments in which it was 200°C, are marked by * and /. In the third "hot" experiment (/), the specimen was kept at temperature for the relatively long duration of 6 hours.

Table 1

$\Delta\ell$(mm) for underset and overset machine-riveting

Specimen number			*	*				†			
131	1.9	0.5	0.6	1.0	1.3	0.4	0.9				
132	-0.9	-0.9	-1.4	-1.7	-0.4	0.0	0.9				
133	-1.8	-1.8	-2.4	-2.4	-1.3	-1.8	-1.4				
134								-1.3	-0.9	-2.2	-1.3
135								-1.7	-2.2	-3.4	-1.8
136								0.0	0.0	-0.8	-1.8
141		1.9	0.2	0.2	2.2	1.8	1.4	1.3	2.2	0.6	2.2
142	2.4	1.4	0.4	0.2	1.8	1.4	0.9				
143	2.9	1.9	1.9	1.4	2.7	2.8	2.3				
144								2.2	2.8	1.7	2.3
145								0.4	0.4	-1.2	-0.9

The most striking result is that $|\Delta\ell|$ for all specimens is less than 3 mm. The thermal contact of the lap-joints is therefore good, even though the setting of the rivets is outside the limits that would be passed, by visual inspection, for mechanical soundness.

Not all the scatter of these results is attributable to the variability of riveting: in these experiments, small pieces of adhesive glass-cloth tape were used to improve the mechanical strength of the thermocouple welds; radiation losses from the thermally "black" tape may have introduced additional variability.

In spite of the scatter, certain interesting deductions can be made from these results. The average values of $\Delta\ell$ are shown in Table 2; the "normal" experiments are those for which the hot block temperature was about 100°C, compared with 200°C for the "hot" experiments.

Table 2

Average values of $\Delta\ell$ (mm)

	Underset rivets	Overset rivets
normal experiments	-0.64	1.77
hot experiments	-1.17	0.60

It can be seen from Table 2 that the joint conductance is better in the hot experiments and is better for underset rivets. The latter is perhaps surprising; at first glance, it might be expected that increasing the riveting pressure might improve the contact. However, it is suggested in Section 1 that the use of excessive closing pressure would distort the sheets and worsen the contact for regions of overlap away from the rivets. This is discussed in Section 5.

Table 3 gives the results of later experiments, in which the improved method of attaching thermocouples was used (see Appendix B).

Table 3

$\Delta\ell$ (mm) for underset and overset machine-riveting

Specimen number					Average $\Delta\ell$
132			-4.0	underset	-1.96
133	-2.2	-2.0			
135	-2.0	0.4			
141			0.6	overset	-0.13
144			1.2		
145	-0.7	-1.6			

With these experiments, there is some doubt of the validity of the numerical values due to an inadvertant annealing of the hot ends of the specimen which caused an increase in the thermal and electrical conductivities. However, they show the same dependence of $\Delta\ell$ on riveting pressure as Table 2.

4.1.2 Hand riveting

Results, obtained with similar samples (pattern A of Fig.1) joined by hand set rivets (normal setting; pneumatic hand-gun), are shown in Table 4.

Table 4

$\Delta\ell$ (mm) for hand riveting (normal setting)

Specimen number	Length of overlap				Average $\Delta\ell$
111	$\frac{1}{2}$"	-1.3	-1.8		-1.91
112	$\frac{1}{2}$"	0	0		
113	$\frac{1}{2}$"	-3.1	-3.6	-3.6	
114	1"	-2.6	-2.2		-1.90
115	1"		-0.9		

For 1" overlap, the results are similar to those obtained with underset machine-riveting (see Section 4.1.1). The lack of dependence of the average $\Delta\ell$ on the length of overlap suggests that negligible heat transfer between strips occurs in the regions of overlap away from the rivets. With such small numbers, and showing such a large scatter, the apparent numerical agreement is perhaps fortuitous, but later results (see Sections 4.1.3, 4.2.1 and 4.3.1) also support this conclusion.

4.1.3 Final results for standard riveting patterns

Three batches of 20 swg L72 specimens were prepared by maching-riveting (normal setting) to patterns C, D and E of Fig.1. It is considered that pattern C forms a representative test section of two large sheets joined by a single row of rivets; similarly patterns D and E represent large sheets fastened by double rows of rivets.

The results obtained with pattern C specimens is given in the "initial $\Delta\ell$" column of Table 6; the average value of $\Delta\ell$ = 0 mm: this is compared, in Table 5, with the measured $\Delta\ell$ values for double rows of rivets.

Table 5

$\Delta\ell$ (mm) for standard riveting patterns

Rivet pattern	Specimen number	$\Delta\ell$ (mm)
C	231-245	0
D	251	-6.8
	252	-6.8
E	255	-6.0
	256	-7.7
	258	-7.5

The reduction in $\Delta\ell$ obtained by using a double row of rivets is consistent with the suggestion (see Sections 4.1.1 and 4.2.1) that the overlap regions away from the fasteners contribute little to the heat transfer across a lap-joint; use of a second row of rivets produces additional area of good thermal contact in regions of overlap that had previously been in poor contact.

4.1.4 Effects of temperature and temperature cycling

$\Delta\ell$ was measured for specimens of 20 swg L72 strips riveted to pattern C of Fig.1 by machine (normal setting). The specimens were divided into

5 batches and each batch was given a different thermal treatment; $\Delta\ell$ was then measured again. The results are shown in Table 6.

Table 6

Effects of temperature and temperature cycling

Batch number	Specimen number	Initial $\Delta\ell$ (mm)	$\Delta\ell$ after treatment	Storage time (days)	Oven temperature
1	241	-0.3	0.2	270	room temperature
	242	-0.4	-0.6		
2	243	-0.3	0.4	38	50°C
	244	-0.1	-0.4		
	245	0.2	0.2		
3	237	0.4	0.4	40	80°C
	238	0.6	0.1		
	239	-0.5	0.2		
4	231	0.2	0.5	33	110°C
	232	0.3	0.2		
	233	0	0.4		
5	234	-0.4	0.1	33	110°C
	235	-0.3	0.1		
	236	0.6	0.2		
		average = 0			

The specimens of batch 5 were removed from the oven and allowed to cool, twice daily. It is concluded from these results that the effects of the temperatures used, and of temperature cycling, on $\Delta\ell$ is negligible.

4.2 Bolted L72 lap-joints

4.2.1 Bolted L72 lap-joints with 4 lb in fastening torque

The values of $\Delta\ell$ (mm) obtained with 3 cm wide strips of 20 swg L72, joined with two 6 BA stainless steel nuts and bolts (pattern A of Fig.1), are given in Table 7. The length of the overlap was 1". Drilling burrs were carefully removed, and the bolts were tightened using a 4 lb in torque-spanner.

Table 7

$\Delta\ell$ (mm) for bolted L72 lap-joints (pattern A)

Specimen number			
211	-9.6	-4.8	-3.5
212	-3.7		
213	0		-1.8
214	0	-0.4	0
215	-8.8	-5.7	-5.7
216	-0.9	-2.6	-2.2

The temperature of the hot block was about 100°C and that of the cold sink about 20°C. Adhesive glass-fibre tape was again used to anchor the thermocouple wires, but with these samples a smaller area of tape was used to reduce radiation losses. Using additional thermocouples, it was found that the temperature distribution along the strips was uniform - indicative of negligible radiation loss (see Appendix D).

As with riveted specimens, the thermal conductance of all joints was good; the average of the values in Table 7 is $\Delta\ell$ = -3.31 mm. Comparison with Tables 2, 3 and 4 (see Sections 4.1.1 and 4.1.2) show that, in general, bolted joints are slightly better than riveted joints; but the scatter of individual values - both between specimens and for repeated observations on the same specimen - is slightly larger.

A single specimen (number 291), made from strips of 20 swg DTD 610 (similar to L72), had three rows each of two 6 BA screws (4 lb in torque-spanner) in a 1" overlap. The measured $\Delta\ell$ was -5.2 mm. The improvement, compared with a single row (Table 7), is smaller than that obtained using a second row of rivets (Table 5, Section 4.1.3). This is discussed in Section 5.

4.2.2 The effect of fastening torque

The effect of bolting pressure was studied using samples made to pattern B of Fig.1. A single 6 BA stainless steel nut and bolt was used to fasten the 18 swg L72 strips; the width of the overlap was $\frac{1}{2}$" and the overlap length was 1 cm. Torque-spanners were used to tighten the nuts and bolts. A spot of "Durofix" was used to provide a less radiative anchorage for each thermocouple wire. The results are shown in Table 8.

Table 8

$\Delta\ell$ (mm) for bolted L72 lap-joints (pattern B)

Specimen number	Torque lb in			*	
411	1.7	0.9	1.1	0.1	0.7
412	2.0	0.2	0.3	-0.2	0
413	3.0	-0.3	-0.2	-1.4	-0.5

In the experiment marked *, the top block temperature was about 200°C compared with about 100°C for the other three experiments: in all experiments the cold sink temperature was about 20°C.

The results show that increasing the bolting torque increases the thermal conductance of the lap-joint, that is apparently the opposite effect to that obtained with increasing the riveting pressure (see Section 4.1.1). This is discussed in Section 5.

In a later experiment two specimens, made to pattern A of Fig.1, were each fastened with two 6 BA stainless steel nuts and bolts using a 9 lb in torque-spanner - the breaking torque is slightly greater than 10 lb in. A slight distortion of the strips to form a slight surface depression around the fasteners was produced. The appearance was similar to that produced by under-set riveting. The measured values of $\Delta\ell$ are shown in Table 9.

Table 9

$\Delta\ell$ (mm) for bolted L72 lap-joints (pattern A) - high torque

Specimen number	9 lb in	3 lb in
271	4.7	5.3
272	6.0	5.4

Comparison with Table 7, shows that the use of a 9 lb in torque-spanner produces a poorer contact than 4 lb in. Unfastening the bolts and re-tightening to 3 lb in did not improve the contact (last column of Table 9) suggesting that the effect of the high torque was to produce a permanent deformation.

4.3 Effects of surface hardness and roughness

4.3.1 Bolted L70 lap-joints

L70 material is essentially unclad L72. The Brinell hardness is 125 compared with 16 for pure annealed aluminium. From the discussion in Section 1,

on the microjunctions that form the metallic conduction paths for heat transfer between the two strips of a lap-joint, it is to be expected, for a given contact pressure, that the soft aluminium cladding of L72 sheet would lead to a larger area of true contact, and hence a lower thermal resistance, than occurs with L70 (see Section 5). Comparison of $\Delta\ell$ obtained with L70 and L72 specimens confirms this.

The values of $\Delta\ell$ (mm) obtained with 3 cm wide lap-jointed strips of 18 swg L70 are given in Table 10; each joint (pattern A of Fig.1) was fastened with two 6 BA stainless steel screws and nuts using a 4 lb in torque-spanner; the overlap length was 1".

Table 10

$\Delta\ell$ (mm) for bolted L70 lap-joints

Specimen number					≠	≠	≠
311	2.9	3.4	3.3	3.3			
312	1.4	0	0.5	0.9			
313	1.0	0.5			0.9	1.4	
314	-1.0	-0.6	-0.5				0.5
315		-0.5			0.5	0.5	
316	1.0	1.9	0.5				2.9

In Table 10, the first 4 columns of results are for successive experiments; between runs the apparatus was cooled to room temperature, air was admitted and the apparatus re-evacuated. The average of all values in these 4 columns is $\Delta\ell$ = 1.06 mm. Comparison with the average value, $\Delta\ell$ = -3.31 mm (Section 4.2.1) obtained with similar lap-joints of L72, shows the increased thermal conductance resulting from the aluminium cladding.

On two of the specimens (numbers 313 and 315), the screws were slackened after the second experiment and re-tightened gently; a torque-spanner was not used - the estimated torque was about 2 lb in, but certainly less than the original 4 lb in. The effect of this, shown in the columns marked by ≠, was to increase $\Delta\ell$ slightly. In later experiments (see Section 4.2.2) the effect of bolting torque was studied more carefully.

In addition, the length of overlap for two specimens (numbers 314 and 316) was reduced from 1" to $\frac{3}{8}$" by removing 5/16" of the unfastened free end

from each strip; the column marked by $\neq$ shows that this increased $\Delta\ell$ slightly. Comparing the effective lengths of two strips - the one having a 1" overlap length, the other $\frac{3}{8}$", but both having the same overall length - the reduction in effective length, and therefore the contribution to the heat transfer, due to the additional 5/8" of unfastened overlap is seen to be quite small. Thus, for specimen number 314, the effective length of the overlap is $a + \Delta\ell = \frac{3}{8}" + 0.02"$; adding 5/8" gives 1.02" for the effective length of a 1" length of jointed strip containing a $\frac{3}{8}$" overlap: this is about 4% greater than the effective length, 1" - 0.02" = 0.98", for the same specimen with a 1" overlap. Specimen number 316 gives a similar result. This gives experimental confirmation of the suggestion in Section 1, that most of the heat transfer occurs close to the fastener.

4.3.2 Indium interlayers

In view of the improved thermal contact obtained with the soft aluminium clad L72, it might be expected that the use of a thin layer of soft metal between the overlapping strips would lead to a further improvement. However, the resistance of the additional interface introduced by the use of such an interlayer may vitiate this. The effect of interposing 0.006" indium foil (Brinell hardness = 1) was studied using $\frac{1}{2}$" wide lap-jointed strips of 18 swg L72 (pattern B of Fig.1) with an overlap length of 1 cm; the 6 BA stainless steel nut and bolt was tightened using a 2 lb in torque spanner. The values of $\Delta\ell$ obtained are given in Table 11.

Table 11

$\Delta\ell$ (mm) for bolted L72 lap-joints with indium interlayer

Specimen number	*		
411	-2.0	-2.9	-2.4
412	-1.6	-2.7	-2.2
413	-1.6	-2.5	-2.0

The first column of results was obtained with temperatures of about 100°C for the hot block and about 20°C for the cold sink. Before inserting the indium foil, we had obtained $\Delta\ell = 0$ for specimen number 412 for a fastening torque of 2 lb in (Table 8 of Section 4.2.1). It is clear, therefore, that the insertion of indium foil increases the heat transfer in spite of the extra interface introduced.

Increasing the temperature of the hot block to about 190°C, and the indium to about 130°C, improves the joint conductance (column of results marked by *) and part of this improvement is retained on reducing the hot block temperature to about 100°C again (final column). The possibility that this improvement is due to some diffusion and alloying or welding is supported by the signs of adhesion that were found on dismantling one of the specimens.

4.3.3 The effect of burrs

It has previously been stressed (Section 2.1) that, in preparing the specimens, any burrs, raised in drilling the clearance holes for the fasteners, were carefully removed before the strips were assembled. It was believed that failure to do this would produce a lap-joint with poor thermal conductance since the contact would be extremely localized and there would be no contribution to the heat transfer from the remaining large area of overlap. This was studied using 3 specimens (pattern A of Fig.1) of 3 cm wide 18 swg L70; the burrs were not removed and the strips were assembled with the burrs facing each other. The two 6 BA stainless steel nuts and bolts were tightened using a 1.7 lb in torque-spanner. The gaps between the strips, produced by this clearly uncontrolled procedure, were about 0.002" or less. A fourth specimen (number 315) had a symmetrical pattern of 10 small pimples raised on each strip by mechanical indentation; the strips were then assembled with the pimples facing each other to give 10 localized contact areas. The results obtained in "normal" temperature (hot block ~100°C; cold sink ~20°C) experiments is given in Table 12.

Table 12

$\Delta\ell$ (mm) for bolted L70 specimens - burrs not removed

Specimen number	Overlap length	1.7 lb in	1.7 lb in	4.0 lb in
331	$\frac{1}{2}$"	6.4	6.3	
332	$\frac{1}{2}$"	9.2	10.0	
333	1"	9.5		7.1
315	1"	7.4		3.8

Comparing these results with those of Table 10 (Section 4.3.1) shows that failure to remove burrs results in lap-joints having significantly higher resistance.

4.4 Miscellaneous factors: electrically insulating joints

In the transfer of heat between the strips of a bolted lap-joint, there is, in addition to the metallic conduction paths formed by the microjunctions at the interface, a path through the head of the screw, its shank and the nut. In order to estimate the relative importance of this route, a few specimens with insulated screws were tested. Later, specimens having insulating interlayers were used (a thermally conducting, but electrically insulated, joint is perhaps relevant to the attaching of transistors to their heat sinks). In these experiments, the specimens were all 3 cm wide, 18 swg L70, with 1" overlap (pattern A of Fig.1).

The effects of interlayers of anti-corrosion fluid and of high emissivity paint were also studied.

4.4.1 Insulated screws

Specimen 321 had enlarged holes to accommodate thin sleeves of silicone-rubber covering the shanks of the 6 BA stainless steel screws. Ceramic washers were placed under the nut and the head of the screw to increase considerably the thermal resistance of the conduction path via the fastener. This specimen was compared, in two successive experiments, with two specimens (322 and 333) having normal 6 BA clearance holes and non-insulated screws; the estimated bolting torque was $\frac{1}{2}$ 2 lb in. In a third experiment (marked by $\not$), the ceramic washers were removed from specimen 321 and the three specimens were re-assembled using a 1.7 lb in torque-spanner. The results are shown in Table 13.

Table 13

$\Delta\ell$ (mm): heat transfer via the fastener

Specimen number			$\not$
321	2.9	2.3	4.4
322	1.4	1.8	1.4
333	1.5		0.8

The results are not conclusive; but the smallness of the difference in $\Delta\ell$ suggests that conduction across the interface is much more effective than that via the fastener.

4.4.2 Electrically insulated lap-joints

The values of $\Delta\ell$ obtained in experiments with electrically insulated joints are given in Table 14.

Table 14

Electrically insulating joints

Specimen number	screws	Torque lb in	interlayer	$\Delta\ell$ (mm)
312	nylon	~1	none	15.9
313A	nylon	~1	none	7.0
313	nylon	~1	fluon	37.6
321A	steel	4	mica	73.2
321C	steel	3	mica	77.1
321B	steel	4	anodized Al	8.2

The stainless steel fasteners were electrically insulated from the L70 strips by having mica washers under the nuts and screw-heads and by passing through enlarged clearance holes without touching. Both the fluon tape and the mica interlayers were 0.004" thick. With specimen 321B, the insulating interlayer consisted of two strips of anodized aluminium (3.2 cm × 1.1 cm, thickness 0.022"; anodic oxide coating 0.0001") placed each side of the line of the bolt-holes. The electrical resistance of the insulated joints was greater than 20 MΩ.

The results show that the clamping load available with nylon screws is inadequate to provide good thermal contact between L70 strips, and that for producing high thermal conductance with electrical insulation, anodic aluminium oxide coatings are much better than mica interlayers.

4.4.3 Anti-corrosive jointing compound

The effect of anti-corrosion fluid ("Celloseel") was studied using specimen number 223. Two 3 cm wide, undrilled, strips of 20 swg L72 were coated with fluid and placed together to form a lap-joint with a 1" length of overlap. The joint was pressed together under a 1 lb load and air-dried for 18 hours at room temperature, followed by 25 hours at 60°C. The electrical resistance of the joint was a few ohms - not high enough, perhaps, to preclude the possibility of there being some slight metallic contact through the layer of compound.

Tested under "normal" conditions, $\Delta\ell$ was -8.1 mm and -8.4 mm in successive experiments - the highest thermal conductance joint observed.

Specimen 223 was the only sample tested in which isolated fasteners were not used; it was therefore, the only joint for which one might expect uniform thermal properties over the whole of the interfacial area. The value of ℓ_o/a, corresponding to $\Delta\ell$ = -8.1 mm, is 0.68. Hence, we have, using the analysis of Appendix C and Fig.8, $h \simeq 0.08$ cal sec^{-1} cm^{-2} deg C^{-1} for $k = 1/3$ cal sec^{-1} cm^{-1} deg C^{-1}.

Thus this relatively low value of heat transfer coefficient produces a joint with good thermal conductance with $\ell_o/a = 0.68$; Fig.8 shows that, for $z > 2$ (say), quite large increases in h reduce ℓ_o/a only slightly; even for $h = \infty$, ℓ_o/a is reduced to only 0.5.

4.4.4 The effects of paint layers

The dominant mode of heat transfer inside a satellite is by radiation (see Section 1). With highly reflecting aluminium surfaces, radiative heat transfer coefficients are small. The emissivity can be increased conveniently by using suitable paints. At about room temperature, the maximum of the radiation intensity occurs at a wavelength of about 10 μ; for such long wavelengths the emissivities of paints are high and not strongly dependent on the particular colour of the paint.

The thermal conductance of 4 painted specimens was measured in order to assess the effects of lap-joint assembly after painting - a possibility that might arise if electronic packages in a satellite are changed.

The specimens were made to pattern C of Fig.1 (length of overlap 5/8"): 1½" wide strips of 20 swg L72 were fastened with three 6BA stainless steel screws and nuts, tightened with a 3 lb in torque; only one strip of each specimen was painted, the other was unpainted.

The paints used were to DTD 5555 and were supplied by Cellon-Docker, Kingston-on-Thames. An etch-priming coat (SL.5539 primer + SL.5460 catalyst) was sprayed onto the freshly degreased strips, air-dried for 4 hours and then stove-dried for 1 hour at 80°C. On top of this, a double-track, gloss white, finishing coat (SL.5459 gloss white paint + SL.5460 catalyst) was applied. This coat was also air-dried for 4 hours and stove dried at 80°C for 1 hour. The total thickness of the dried paint film was 0.004".

The painted strips of specimens 261 and 262 were masked for painting so that two strips of paint, parallel to the line of bolt holes, were made on

each strip. Removal of the masking tape produced "steps" at the edges of the paint film. When the specimens were assembled these steps came just inside the overlap area. The central region of the overlap was free of paint so that metallic contact was made where the screws were tightened.

The values of $\Delta\ell$ obtained in "normal" temperature experiments are listed in Table 15.

Table 15

$\Delta\ell$ (mm) for painted specimens

Specimen number	$\Delta\ell$ (mm)
261	0.8
262	1.2
263	18.3
264	16.2

The results show that a continuous film of paint increases considerably the thermal resistance of the interface. Comparing these results with those of Section 5.1, for riveted L72 to the same pattern, shows that stripes of paint, that allow metallic contact in interfacial regions close to the fasteners, affect the thermal conductance only slightly.

5 DISCUSSION

In this section, the results of Section 4 are discussed in terms of the model of interfacial metallic conduction given in Section 1, and the influence on it of using localized fasteners.

We will first estimate the area of real contact for the specimens of Section 4.3.1 (L70; pattern A). As regards the friction between threads, it was found, for a 6 BA nut and screw, that a torque of about 1.5 lb in is required to lift a 100 lb load hanging vertically from the screw. Hence

$$\text{load (lb)} \simeq 60 \times \text{torque (lb in)}$$

after making a small allowance for the friction of the bearing surfaces when the two sheets are bolted together; i.e. for a torque of 4 lb in the load $\simeq$ 240 lb = 108 kgm. The Brinell hardness of L70 is 125 kgm mm^{-2};

hence, neglecting work-hardening of the deforming asperities, the area of real contact is probably of the order of 1mm^2 per bolt - a very small fraction of the 760 mm^2 overlap area. For aluminium-clad L72, the area of real contact is a few mm^2 per bolt; the Brinell hardness of annealed aluminium is 16, but may perhaps be doubled by work-hardening.

Comparison of the results for L72 (Table 7, Section 4.2.1) and L70 specimens (Table 10, section 4.3.1) shows that the presence of aluminium cladding reduces the thermal resistance. A similar reduction is obtained (see Section 4.3.2) by interposing a thin layer of indium (hardness ~ 1kgm mm^{-2}), but in this case the situation is complicated by the introduction of an extra interface.

No systematic study was made of the effects of surface finish: all the specimens tested, except those of Section 4.3.3, had surfaces in the "as received" condition; however care was taken to ensure that the surfaces were not scratched or damaged. Apart from effects due to the dependence of hardness on plastic strain, the area of real contact for a given load is independent of the number of contact points - the product of hardness and area is equal to the load. Comparison of the results obtained with specimens having burrs and the dimpled specimen (Section 4.3.3) with those for similar specimens with burrs removed (Section 4.3.1) shows that gross surface roughness produces high resistance joints. This is consistent with the generally accepted predictions and experiments that a lower thermal resistance is obtained with a large number of small area contacts, i.e. the conductance increases with the surface finish.

In Section 1 it was suggested that the fastening of lap-joints with rivets or bolts would produce intimate contact only in localized regions close to the fasteners, and that, in more remote regions of the overlap, the metallic contact and hence the interfacial heat transfer in the absence of radiation and fluid conduction would be poor; the use of excessive closing pressure would distort the strips and cause them to separate away from the fasteners. It is therefore expected that gradually increasing the closing pressure would first improve, then produce an optimum, and finally worsen the joint conductance; that an increase in the overlap area would cause only a slight improvement; that interposing an insulating layer of paint, in regions away from the fasteners, would cause only a slight worsening; and that the use of multiple rows of fasteners would enable a greater fraction of the overlap

area to contribute effectively to the transfer of heat across the interface. In general, the results of Section 4 support these predictions.

With riveted specimens there is visual evidence of surface depressions around the rivets; this distortion is probably not due to the tension in the rivet itself, but to pressures involved in the riveting process. Comparison of Tables 3 and 4 suggests that the optimum riveting pressure is about that of underset or normally set rivets. Table 4 also shows that a change of overlap area has no effect on $\Delta\ell$, suggesting, for closing pressures sufficient to produce visible surface deformation near the rivet, that the strips are separating. Table 5 shows that a double row of rivets produces a significant improvement.

With bolted specimens, there is a gradual improvement of thermal contact with bolting torque (Table 8); the 4 lb in torque used for the results of Table 7 is probably close to the optimum: an excessive 9 lb in torque (Table 9) produced visible deformation and a joint of poor thermal contact. (In view of the excessively large value of $\Delta\ell$, this result should, perhaps, be discounted; the results obtained after slackening the bolts and retightening to 3 lb in suggests permanent distortion of the specimens.) Table 10 shows a 4% increase in $\Delta\ell$ for a 5/8" reduction in the length of overlap; it is concluded that with a 4 lb in bolting torque there is a small contribution from an extra overlap, in comparison to a zero contribution with visibly deformed riveted specimens. The effect of paint at the edges of the overlap area (Table 15) again suggests a small, but greater than zero, contribution from an extra overlap. As with rivets, multiple rows of bolts (Section 4.2.1) produce a significant improvement in joint conductance.

The thermal conductance of the joints increases with temperature (Table 2). The temperature of the centre of the joint is the mean of the hot and cold block temperatures, i.e. about 60°C in a "normal" experiment and about 110°C in a "hot" experiment. No explanation is offerred for this observed temperature dependence of $\Delta\ell$. However, the results of section 4.1.4, and of Tables 1 and 8, show that the effect is reversible; no permanent increase in conductance results from the higher temperature. This suggests that the softening temperature of the deformed asperities is above 110°C and that, even in long times of order 30 days, there is negligible thermal movement of atoms producing a decrease in hardness and an increase in contact area. With indium interlayers (section 4.3.2) part of the increased heat-conduction in a "hot" experiment is retained in a subsequent "normal" experiment.

It is clear from the definition (see Section 3) of the "additional length" parameter that the value of $\Delta\ell$ should be specific to the particular geometry of the lap-joint. Thus, for example, Table 5 shows that $\Delta\ell$ is a function of the number of rows of fasteners used; it is likely that $\Delta\ell$ depends also on the sheet thickness and on the size of the fasteners used - experimental variables not included in this work.

6 CONCLUSIONS

The thermal behaviour of riveted and bolted lap-joints of aluminium alloys (L70 and L72) in vacuum can be summarized as:-

(a) the dominant mode of interfacial heat transfer is by metallic conduction; the contributions from radiation and gaseous conduction are negligible for low emissivity aluminium surfaces in pressures below 10^{-4} torr (Appendix D).

(b) most of the heat transfer occurs close to the fasteners; the thermal contact in overlap regions away from the rivets or bolts is poor (Sections 1 and 5).

(c) the concept of a uniform heat transfer coefficient is invalid for riveted or bolted lap-joints; the thermal behaviour of the lap-jointed specimens used is better described in terms of an additional length $\Delta\ell$, to be added to the conduction path to allow for interfacial resistance (Section 1). Limitations to the general use of the $\Delta\ell$ parameter are discussed in the final paragraph of Section 5.

(d) for joints of good thermal conductance, $\Delta\ell \simeq 0$; i.e. the effects of interfacial resistance and doubled thickness cancel each other; for a perfect joint $\Delta\ell = -a/2$, where a is the length of overlap (Section 3 and Appendix C).

(e) to produce thermally good joints, the mating surfaces should be flat, and free from scratches and gross surface irregularities; burrs raised in drilling clearance holes for bolts or rivets should be carefully removed (Section 4.3.3).

(f) standard riveting techniques to pass standard visual inspection for mechanical soundness as practised by the aircraft industry (Appendix A) produce joints that are thermally good (Section 4.1).

(g) good joints are also produced by bolting provided that the bolts are tightened properly, but not excessively (Section 4.2).

(h) an improvement in thermal conductance is obtained if multiple rows of fasteners are used (Sections 4.1.3 and 4.2.1).

(i) the thermal contact is improved if the aluminium alloy sheets are clad with pure aluminium (Section 4.3.1).

(j) the thermal conductance increases with temperature (Table 2); temperature cycling and prolonged storage at 110°C have no effect (Section 4.1.4).

(k) a thin indium interlayer improves the thermal contact and a further improvement is obtained after heating to 110°C (Section 4.3.2).

(l) a single experiment suggested that a thin film of anti-corrosive jointing compound ("Celloseel") may not be harmful and may be beneficial (Section 4.4.3).

(m) insulating interlayers of fluon tape, mica and paint, prevent metallic contact and reduce the thermal conductance of the joint (Sections 4.4.2 and 4.4.4).

(n) anodic aluminium oxide coatings can be used to produce electrically insulating joints of only slightly reduced thermal conductance (Section 4.4.2).

ACKNOWLEDGEMENTS

The authors are grateful to Mr. Blondstein (British Aircraft Corporation Ltd., Stevenage) and his colleagues on the U.K.3 satellite project, for their helpful co-operation, and to their skilled craftsmen for riveting and painting some of the specimens.

Appendix A

RIVETING - STANDARD AIRCRAFT PRACTISE

Aluminium alloy rivets are usually* made from L86, which contains 2% copper. Since this alloy does not age-harden appreciably, the rivets can be used from stock without re-annealing. Rivet holes are jig-drilled about 0.002" oversize and burrs are removed. The sections are clamped together and rivets are inserted. With thin sheets the technique of "reaction riveting"is used; a small metal anvil ("dolly") is held against the rivet shank while a second operator presses a hand "gun" lightly against the pre-formed head of the rivet. The hand-gun has a cylindrical steel hammer shaft, pneumatically vibrated along its axis. Under the impact pressure of the vibrating hammer, the rivet shank squashes down and spreads to form a barrel-shaped cheese head against the dolly. The operator, by experience, adjusts time and pressure to produce a uniform size of head. Maximum diameter can be checked by a socket gauge, which should be a snug fit.

More precise mechanical control is obtained by machine-riveting, in which the rivet is squeezed by the steady pressure of a pneumatic plunger; the pressure and stroke are adjustable. This process can be used only on sections of work small enough to be manipulated between the jaws of the machine.

Riveting pressure is normally adjusted to give a result of the type B in Fig.4, in which the cheese-head diameter is 50% larger than the shank diameter. Inadequate pressure produces the "underset" rivet (type A) and excessive pressure causes "oversetting" (type C).

When access to both sides of the work is not available a technique of blind, or "pop", riveting is used. Pop-rivets have a hollow shank which is expanded by the wedge action of an inner core. This method tends to be more variable than the previous methods and is avoided when possible; it has not been included in this investigation.

For the experiments reported in Section 4.1, three batches of machine-riveted specimens were prepared, corresponding to types A, B and C of Fig.4. A fourth batch was made by standard hand-riveting technique, using the pneumatic gun. Fig.5 shows a linear relation between the cheese-head diameter and the overall length; it also shows that, although hand-riveting is more variable than machine riveting, the variation rarely exceeds 5%.

---

* Highly stressed joints may use the stronger L37 alloy, containing 4% copper. These rivets must be annealed shortly before use.

Appendix B

Thermocouples

The junction obtained by spot-welding a fine wire of chromel or alumel onto a surface of aluminium is intrinsically weak. Since these alloys have a much higher resistivity than aluminium, they tend to melt completely before the aluminium surface gets hot. If the tip of the welding electrode is flat, the wire collapses under it forming a thin wafer of negligible strength. By use of a rounded or cylindrical electrode surface, a more gradual change of wire thickness, with improved mechanical strength, is obtained.

The wires to be welded should be free from surface oxide; ordinary "black" wire can be cleaned with carborundum paper, but it is more convenient to use bright drawn wire*. Alumel tarnishes slowly in air, but the thin surface film is easily removed. Oxidation of base metals is generally controlled by reducing welding time to a minimum: we therefore tried a capacity power supply, with a discharge time of about 10 m sec ; however, excessive splashing occurred, preventable only by using excessive electrode pressure (a 20 lb load): better results were obtained with a thyratron-controlled power supply, using a longer weld-time (40 m sec = 2 cycles) and normal electrode pressure.

These welds were reasonably strong in tension, but still rather weak under bending stresses. Additional mechanical support was provided by anchoring each wire to the edge of the specimen. For the earliest specimens, a small strip of adhesive glass-fibre tape was used; with later specimens this was replaced by a spot of "Durofix", to reduce radiation losses (see Appendix D).

In order to control the location of the hot junctions (see Fig.6, lines were scribed across the specimens at accurately measured intervals. A pair of wires (diameter 0.012" for the earliest specimens; 0.007" later) was laid end-to-end along the scribe-lines, and individually welded. The scribe-lines were perpendicular to the long axis of the specimens, that is, perpendicular to the direction of heat flow, so that the thermal emf's would be unaffected by the intermediate section of aluminium at each junction.

---

* Obtainable, for example, from A.G. Scott Ltd., Manchester.

Appendix C

THEORY OF THE LAP-JOINTED STRIP IN THE STEADY STATE, EXCLUDING RADIATION AND GAS-CONDUCTION

As discussed in Sections 1 and 5, the use of localized fasteners produces non-uniformities in the thermal resistance across the interface of a lap-joint. A simple description of the thermal behaviour of such joints is provided by the concepts of effective length ℓ_o, and additional length $\Delta\ell$ due to thermal resistance, proposed in Section 3. However, for the case of uniform thermal resistance, the results can be expressed in terms of the usual heat transfer coefficient h, i.e., the heat flux per unit temperature difference across the interface of the overlapping strips. In this appendix, we give, since it is not included in the standard reference books, a theory for this ideal case of constant h.

The conduction of heat in lap-jointed strips (width u; thickness v; thickness 2v in the overlap region $-\frac{1}{2}a \geq x \geq \frac{1}{2}a$ - see Fig.7) is essentially one dimensional for large thermal conductivity k, if v is small enough. In the absence of radiation and at pressures low enough for gas-conduction losses to be negligible, the flow of heat Q is, in the steady state, constant along the specimen.

Let subscript 1 refer to the hotter and subscript 2 to the colder of the two strips. For an element ∂x of the overlap region, the net heat conducted by one strip is equal to the heat transferred to the other strip. Hence, in the steady state,

$$\left.\begin{aligned} kuv\frac{\partial^2 T_1}{\partial x^2} &= hu(T_1 - T_2) \\ kuv\frac{\partial^2 T_2}{\partial x^2} &= hu(T_2 - T_1) \quad . \end{aligned}\right\} \qquad (C.1)$$

Subtracting and adding these equations, and putting $\alpha = T_1 - T_2$ and $\beta = T_1 + T_2$, we obtain

$$\frac{\partial^2 \alpha}{\partial x^2} = \frac{2h}{kv}\alpha = m^2\alpha \qquad (C.2)$$

$$\frac{\partial^2 \beta}{\partial x^2} = 0 \quad . \qquad (C.3)$$

The solutions are,

$$\alpha = C e^{mx} + D e^{-mx} \tag{C.4}$$

$$\beta = Ax + B \tag{C.5}$$

where the constants A, B, C and D are to be found from boundary conditions.

The condition of constant heat flux gives,

$$Q = -k u v \left(\frac{\partial T_2}{\partial x}\right)_{x \geq \frac{1}{2}a} = -k u v \left(\frac{\partial T_1}{\partial x}\right)_{x \leq -\frac{1}{2}a} . \tag{C.6}$$

Since the temperature versus distance diagram is symmetrical and there is no heat flow from the free ends of the strips, we have

$$\left(\frac{\partial T_1}{\partial x}\right)_{x=\frac{1}{2}a} = \left(\frac{\partial T_2}{\partial x}\right)_{x=-\frac{1}{2}a} = 0 . \tag{C.7}$$

Differentiating equation (C.5), we obtain

$$\frac{\partial \beta}{\partial x} = \frac{\partial T_1}{\partial x} + \frac{\partial T_2}{\partial x} = A \tag{C.8}$$

and from equations (C.7) and (C.6),

$$A = -\frac{Q}{k u v} = \left(\frac{\partial T_1}{\partial x}\right)_{x \leq -\frac{1}{2}a} = \left(\frac{\partial T_2}{\partial x}\right)_{x \geq \frac{1}{2}a} . \tag{C.9}$$

Differentiation of equation (C.4) gives

$$\frac{\partial \alpha}{\partial x} = \frac{\partial T_1}{\partial x} - \frac{\partial T_2}{\partial x} = C m e^{mx} - D m e^{-mx} . \tag{C.10}$$

Adding and subtracting equations (C.8) and (C.10), and using boundary condition (C.7), we obtain

$$C = D = \frac{-A}{2m \sinh\left(\frac{1}{2}m a\right)} \tag{C.11}$$

Let T_o be the average temperature at $x = 0$; that is

$$T_o = \tfrac{1}{2}\left\{T_{1(x=0)} + T_{2(x=0)}\right\} .$$

From symmetry,

$$T_o = \tfrac{1}{2}\left\{T_{1(x=-a/2)} + T_{2(x=a/2)}\right\}$$

also, and is thus readily derived from observed temperatures. Substitution in equation (C.5), for $x = 0$, gives

$$B = 2T_o . \qquad (C.12)$$

The complete solutions are, therefore,

$$\left.\begin{aligned} T_1 &= T_o + \tfrac{1}{2}Ax\left[1 - \frac{\cosh mx}{mx \sinh\left(\tfrac{1}{2}ma\right)}\right] \\ T_2 &= T_o + \tfrac{1}{2}Ax\left[1 + \frac{\cosh mx}{mx \sinh\left(\tfrac{1}{2}ma\right)}\right] . \end{aligned}\right\} \qquad (C.13)$$

where A, from equation (C.9), is the temperature gradient $\frac{\partial T}{\partial x}$ in either strip away from the overlap region.

To calculate h, we substitute, in equations (C.13), the temperature drop ΔT across the lap-joint, deduced from observed temperatures using equation (3) of Section 3. As before, division by $-\partial T/\partial x$ gives the "effective length" ℓ_o of an actual length a of overlap. Hence,

$$\frac{\ell_o}{a} = 1 + \frac{1}{a}\left[C\left(\frac{\theta_1 - \theta_2}{\theta_2 - \theta_3}\right) - b\right] = \tfrac{1}{2}\left[1 + \frac{\coth\left(\tfrac{1}{2}ma\right)}{\tfrac{1}{2}ma}\right] . \qquad (C.14)$$

Note that for a perfect "ideal" joint,

$$h \to \infty$$

$$\frac{\coth \tfrac{1}{2}ma}{\tfrac{1}{2}ma} \to \frac{1}{\infty}$$

$$\frac{\ell_o}{a} \to \tfrac{1}{2}$$

that is, the effective length is half the actual length - the expected result since the thickness is doubled at the overlap. For a value of ℓ_o/a, derived from experiment using equation (5), Fig.8, in which $\frac{1}{2}(1 + \coth z/z)$ is plotted against $z(=\frac{1}{2} m a)$, can be used to solve equation (C.14) graphically for m; the heat transfer coefficient h is then given by $h = \frac{1}{2} k u m^2$ (equation (C.2)).

Fig.8 also shows that, for $\ell_o/a \leq 1$, ℓ_o is not strongly dependent on h ($z \propto \sqrt{h}$). From an engineering point of view, this implies that, when ℓ_o has been reduced to $\ell_o \approx a$, only slight advantage is obtained by increasing h further; for example, the results of Section 4.4.3 show that an increase of h from 0.08 cal sec^{-1} cm^{-2} deg C^{-1} to infinity reduces ℓ_o/a only slightly - from 0.68 to 0.5.

Appendix 3

THE EFFECTS OF RADIATION AND GASEOUS CONDUCTION

The steady state temperature distribution, for heat flowing through a long bar from which the sideways heat losses are proportional to the temperature difference $(T - T_0)$ between the bar and its surroundings, is described in the standard theoretical treatments of heat conduction[15,16]. For the particular case of a bar of cross-section uv, thermal conductivity k, and surface heat transfer coefficient ε, we have, in the steady state

$$k u v \frac{\partial^2 T}{\partial x^2} = 2 (u + v) \varepsilon (T - T_0) \qquad (D.1)$$

Writing θ for $(T - T_0)$, we obtain

$$\frac{\partial^2 \theta}{\partial x^2} = \frac{2 (u + v)}{u v} \frac{\varepsilon}{k} \theta = n^2 \theta . \qquad (D.2)$$

The solution is

$$\theta = E e^{nx} + F e^{-nx} \qquad (D.3)$$

where the constants E and F are to be found from boundary conditions.

In the absence of lateral heat losses, the temperature varies linearly with distance along the bar; but if ε is finite the temperature profile is curved. The curvature can be studied by observing the temperatures θ_1, θ_2 and θ_3 at three points on the bar. If the distance between consecutive points is equal (say b), we have, from equation (D.3),

$$\frac{\frac{1}{2}(\theta_1 + \theta_3)}{\theta_2} = \frac{1}{2} (e^{nb} + e^{-nb}) = \cosh nb = \omega \text{ (say)} \qquad (D.4)$$

Hence
$$nb = \cosh^{-1} \omega = \ln [\omega + \sqrt{\omega^2 - 1}] \qquad (D.5)$$

In order to estimate the effects of radiation and gas-conduction on the experiments of Section 2.3, we consider a 25 cm length of unjointed 3 cm x 1/10 cm strip of aluminium alloy ($k \sim 1/3$ cal sec^{-1} cm^{-1} deg C^{-1}) clamped between the two blocks of the apparatus.

The radiant heat flux is given by Stefan's law,

$$Q_1 = E\sigma(T^4 - T_o^4) \qquad (D.6)$$

in which $\sigma = 5.72 \times 10^{-12}$ watts cm^{-2} deg C^{-4} and E is the total emissivity - or emissive power expressed as a fraction of a "black body" - of the surface. Hence the heat transfer coefficient for radiation is,

$$\varepsilon_1 = \frac{dQ_1}{dT} = 4E\sigma T^3 \qquad (D.7)$$

which, for a highly reflecting metal surface ($E \sim 10^{-1}$ say) at 330°K (the mean temperature of the experiments), gives

$$\varepsilon_1 \simeq 2 \times 10^{-5} \text{ cal sec}^{-1} \text{ cm}^{-2} \text{ deg C}^{-1} . \qquad (D.8)$$

For air at 5×10^{-5} torr (the residual pressure in the apparatus) the rate of molecular impacts is about 2×10^{16} cm^{-2} sec^{-1}; taking the specific heat as 6 cal $mole^{-1}$, or 10^{-23} cal $molecule^{-1}$ (5/2R for a diatomic gas plus $\frac{1}{2}$R to take account of the higher impingement rate of the faster molecules) and assuming free molecule flow and an energy accommodation coefficient of unity, we obtain for the surface heat transfer coefficient for gaseous conduction in a pressure of 5×10^{-5} torr,

$$\varepsilon_2 \simeq 2 \times 10^{-7} \text{ cal sec}^{-1} \text{ cm}^{-2} \text{ deg C}^{-1} , \qquad (D.9)$$

which is small compared with the coefficient ε_1 for radiation.

Putting $\varepsilon = 2 \times 10^{-5}$ in equation (D.2) we obtain $n^2 = 12 \times 10^{-4}$, or $n = 3.5 \times 10^{-2}$. Hence, for a separation of d = 3 cm between thermocouples, nd = 0.1 and cosh nd = 1.005, so that, for $\theta_2 \sim 40°C$, the departure from linearity $[\frac{1}{2}(\theta_1 + \theta_3) - \theta_2]$ is about 1/5°C, which is about the limit of sensitivity of the thermometry used (see Section 2.3). In experiments, using specimens with additional thermocouples, no curvature of the temperature profile was detected.

A more sensitive experiment is to raise both copper blocks of the apparatus to the same temperature (~40°C above ambient, say) and to

observe how much cooler the centre of an unjointed strip is. If the temperatures are θ_ℓ at the two ends, $x = \pm\ell$, and θ_o at the centre of the strip, we have, from equation (D.3)

$$\cosh n\ell = \frac{\theta_\ell}{\theta_o}$$

or

$$\theta_\ell - \theta_o = (\cosh n\ell - 1)\,\theta_o \qquad (D.10)$$

For $2\ell = 20$ cm, and taking $n \sim 3.5 \times 10^{-2}$ as before, we obtain $n\ell = 0.44$ and $\cosh n\ell = 1$, giving $\theta_\ell - \theta_o \sim 4^\circ$C. In such experiments, using the earliest specimens which had 0.012" diameter thermocouple wires supported by adhesive glass-fibre tape, the centre was 1 to $1\frac{1}{2}^\circ$C cooler than the ends. This difference was reduced to about $\frac{1}{2}^\circ$C by using 0.007" wires supported by spots of "Durofix" - indicating that the high emissivity of the tape and the relatively large area needed to provide anchorage for the wires were introducing unnecessary radiation losses. This improved thermocouple technique, with the lower radiation loss, was used for the later specimens (see Appendix B); a $\frac{1}{2}^\circ$C temperature difference suggests an emissivity of order 1% rather than the 10% assumed in the sums above. Thus, for the experiments described in Section 2, it is concluded that the heat losses from the sides of the specimens are negligible.

As regards the heat transfer in the overlap region of the lap-jointed specimens, we will now show that, under the conditions of the experiments, the contributions of radiation and gaseous conduction are very much smaller than that of metallic conduction. In most of the experiments $\ell_o/a \simeq 1$ (see Section 4). Assuming, for the purposes of this argument, that the thermal behaviour of the interface can be described in terms of a heat transfer coefficient h, uniform over the overlap region (see Appendix C), we have from Fig.8,

$$z = \tfrac{1}{2} m a = \frac{a}{\sqrt{2kv}}\sqrt{h} = 1.16$$

or

$$h \simeq 10^{-2} \text{ cal sec}^{-1} \text{ cm}^{-2} \text{ deg C}^{-1} \qquad (D.11)$$

which is so large, compared with the radiative heat transfer coefficient, $\varepsilon_1 \simeq 2 \times 10^{-6}$ cal sec^{-1} cm^{-2} deg C^{-1} for 1% of black body, that, even with multiple reflections, metallic conduction must be the predominant mode of heat transfer.

Comparison of equations (D.9) and (D.11) suggests that the transfer of heat across the interface by gaseous and metallic conduction should be equal at a pressure of 2.5 torr. However, the assumptions of free molecular flow and a uniform h, implied in this comparison, are probably invalid. Experiments at higher pressures indicated an increasingly significant contribution by gas-conduction to the interfacial heat transfer, but the large curvature of the temperature profile produced by the increased lateral losses precluded satisfactory interpretation of experiments. In view of this, only a few experiments at higher pressures were attempted and their results are not reported.

REFERENCES

No.	Author	Title, etc.
1	F.P. Bowden D. Tabor	The friction and lubrication of solids. Clarendon Press, Oxford (1950)
2	R. Holm	Electric contacts handbook, 3rd edition Springer-Verlag; Berlin (1958)
3	T.N. Cetinkale M. Fishenden	Thermal conductance of metallic surfaces in contact, general discussion on heat transfer. Proc. Inst. Mech. Engrs., ASME, p 271, (1951)
4	L.C. Laming	Thermal and electrical conductance of machined metal contacts. Ph. D. Thesis, (University of London(1958))
5	H. Fenech W.M. Rohsenow	Prediction of thermal conductance of metallic surfaces in contact. Trans. ASME 85, series C, (62-HT-32) p 15 (1963)
6	R.B. Jacobs C. Starr	Thermal conductance of metallic contacts. Rev. Sci. Instrum., 10, p 140, (1939)
7	Yu. P. Shlykov E.A. Ganin	Experimental study of contact heat exchange. Teploenergetika 8, p 73, (1961) -translation AD 430 088 (28/1/1964)
8	E. Fried F.A. Costello	Interface thermal contact resistance problem in space vehicles. J. Amer. Rocket Soc. 32, p 237, (1962)
9	E. Fried	Thermal joint conductance in a vacuum. ASME paper No. 63-AHGT-18, (March 1963)
10	T.W. McDonald	Thermal contact resistance. Trans. Eng. Inst. Canada 6, (1963)
11	W.E. Kaspareck R.M. Dailey	Measurements of thermal contact conductance between dissimilar metals in vacuum. ASME paper No. 64-HT-38, (August 1964)
12	W. Aron G. Colombo	Controlling factors of thermal conductance across bolted joints in a vacuum environment. ASME paper No. 63-WA-196, (November 1963)

REFERENCES (Contd)

No.	Author	Title, etc.
13	E.H. Coker L.N.G. Filon	A treatise on photoelasticity, 2nd Edition. (Cambridge University Press (1957))
14	I. Fernlund	A method to calculate the pressure between bolted or riveted plates. Report No. 245, Trans. Chalmers Univ. Techn., Gothenberg, Sweden (1961)
15	H.S. Carslaw J.C. Jaeger	The conduction of heat in solids. Clarendon Press, Oxford (1948)
16	H.S. Allen R.S. Maxwell	A textbook of heat, Part 2. Macmillan and Co. Ltd., London (1943)

Fig.1

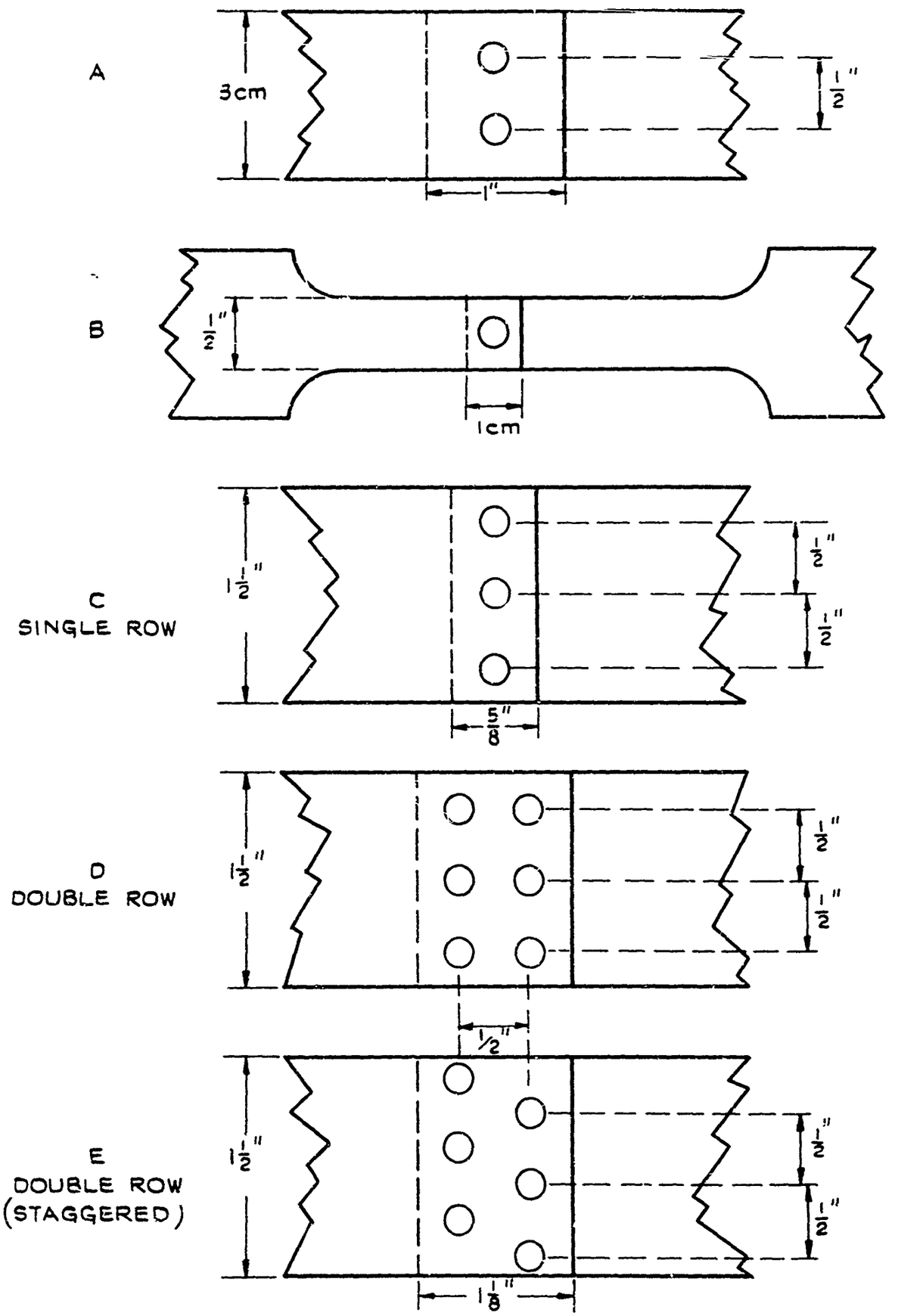

FIG.1 RIVET PATTERNS OF LAP-JOINTED SPECIMENS

Fig.2

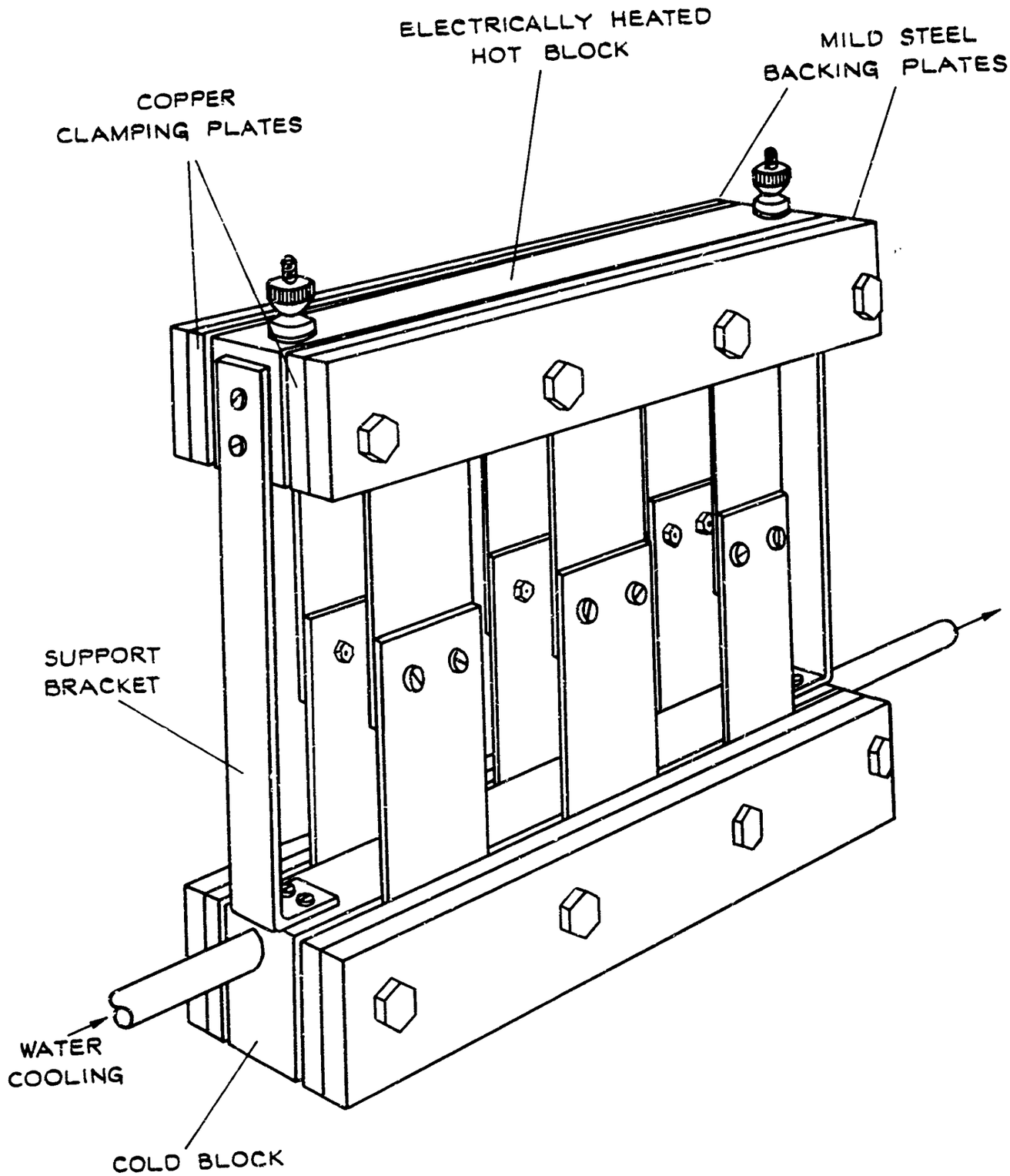

FIG 2 THE APPARATUS

Fig.3

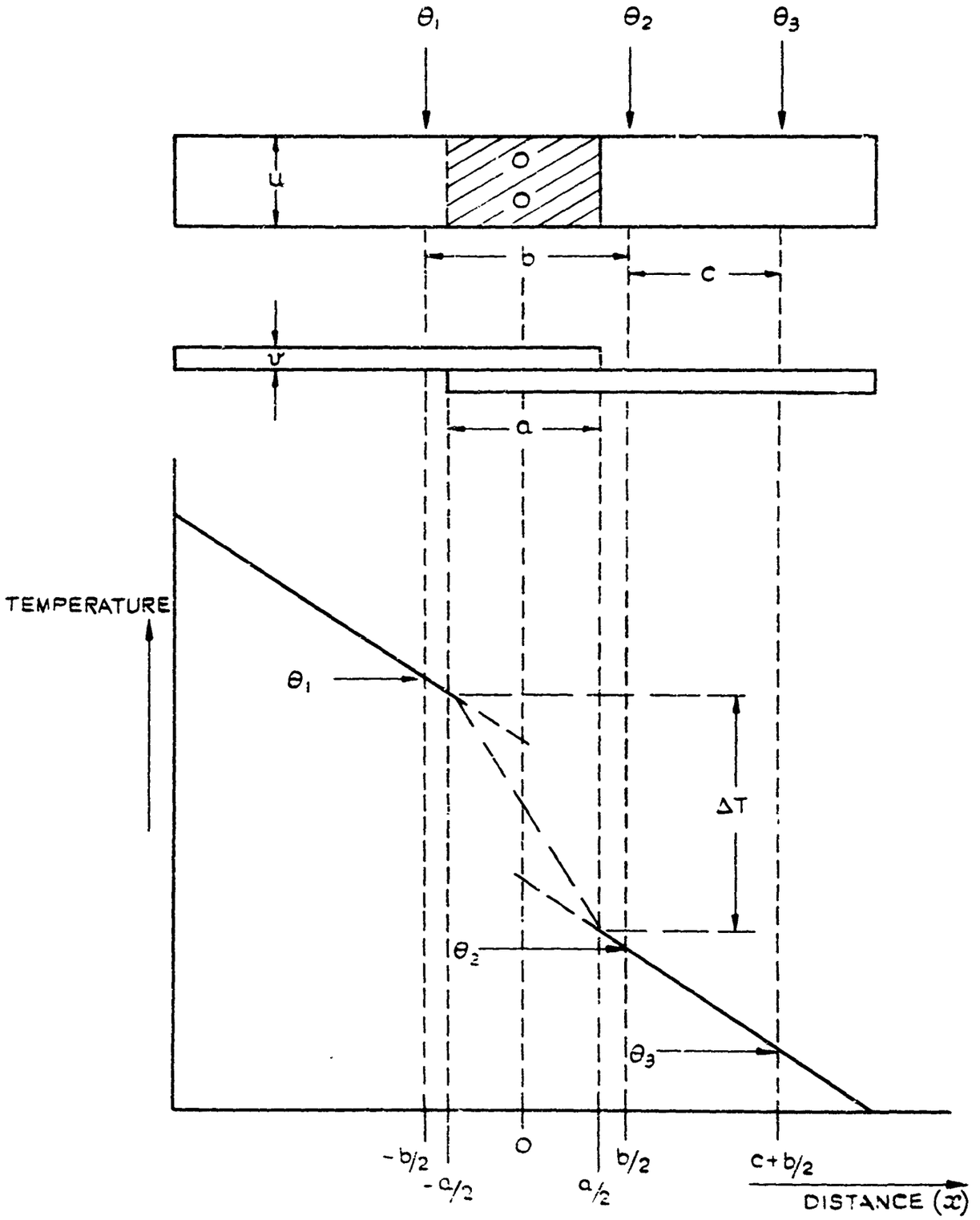

FIG. 3 TEMPERATURE PROFILE OF SPECIMENS

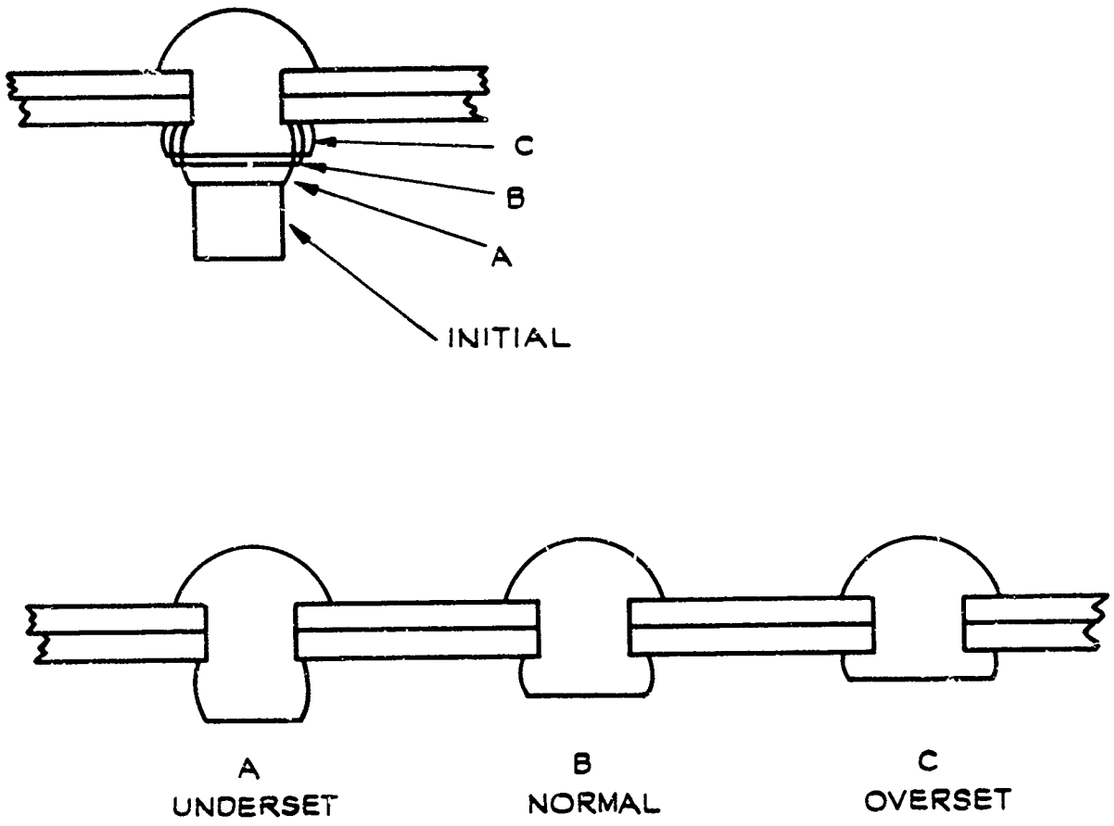

FIG. 4 MACHINE-SET RIVETS

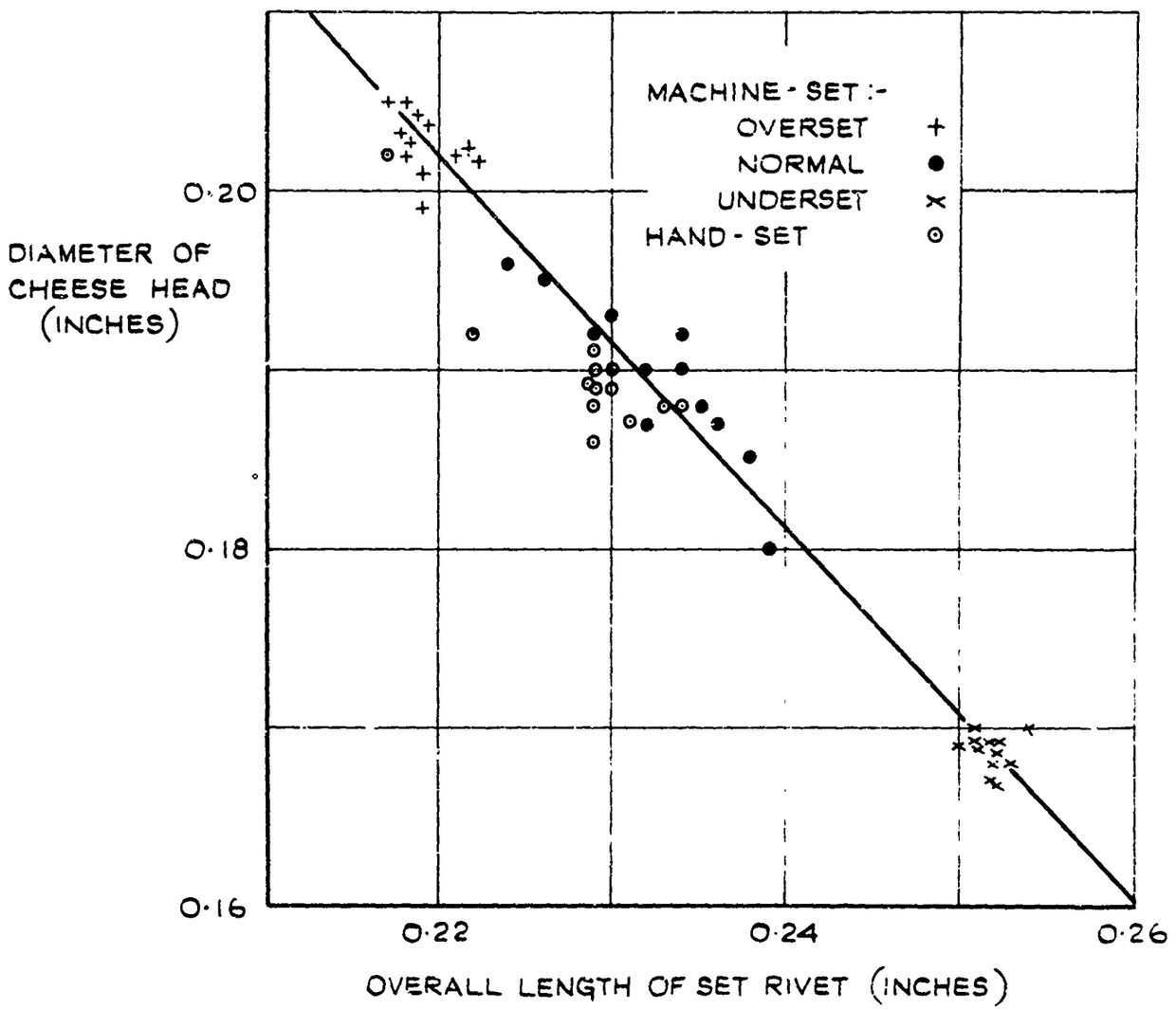

FIG. 5 VARIABILITY OF RIVETING

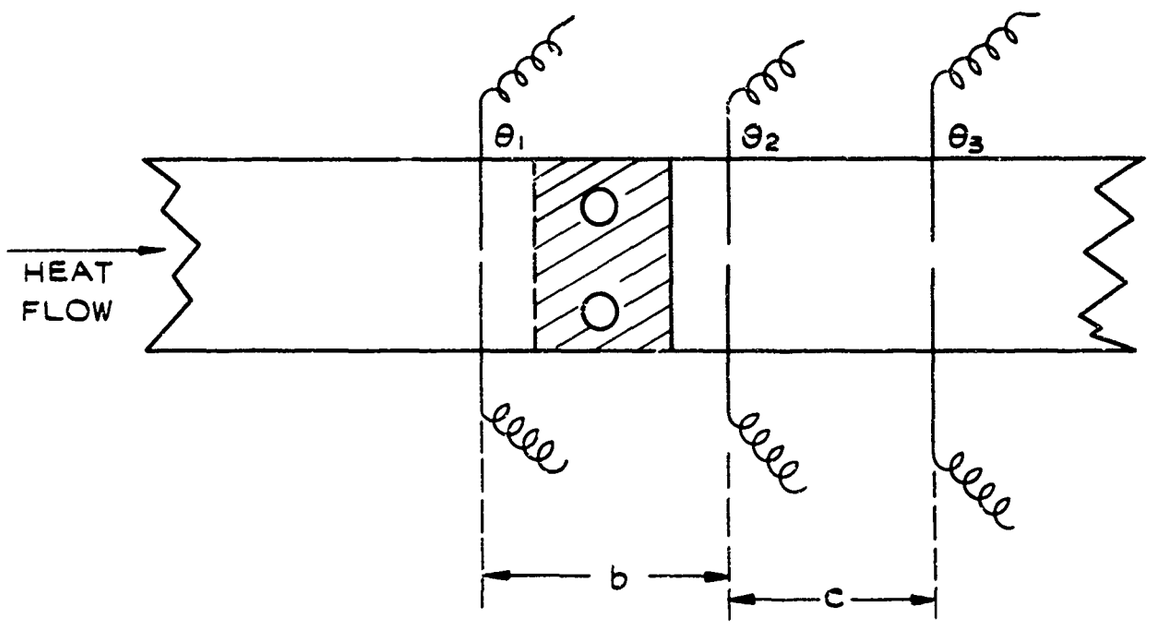

FIG. 6 LOCATION OF THERMOCOUPLES

Fig.7

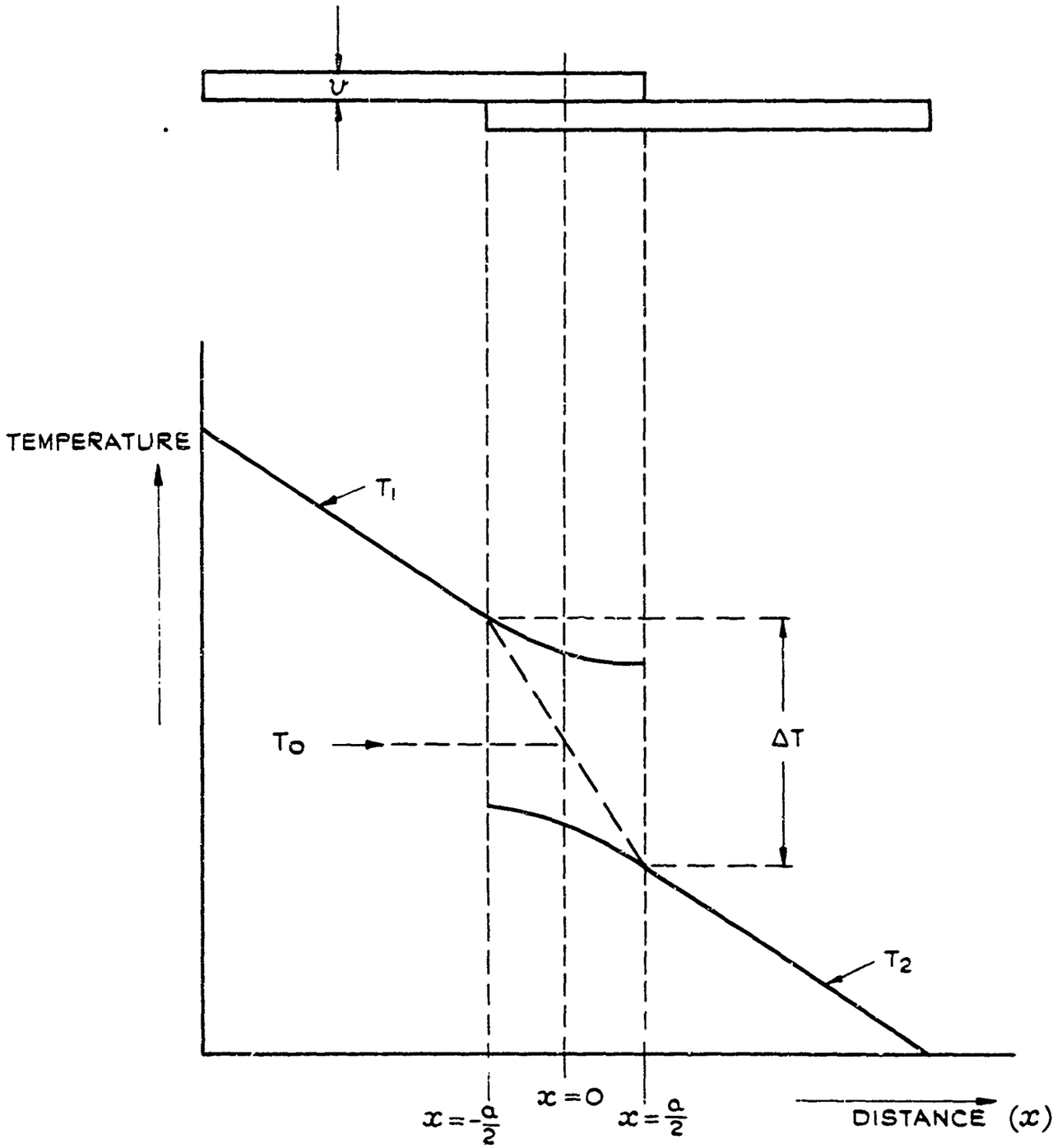

FIG. 7 TEMPERATURE DISTRIBUTION FOR LAP-JOINT WITH UNIFORM h

Fig.8

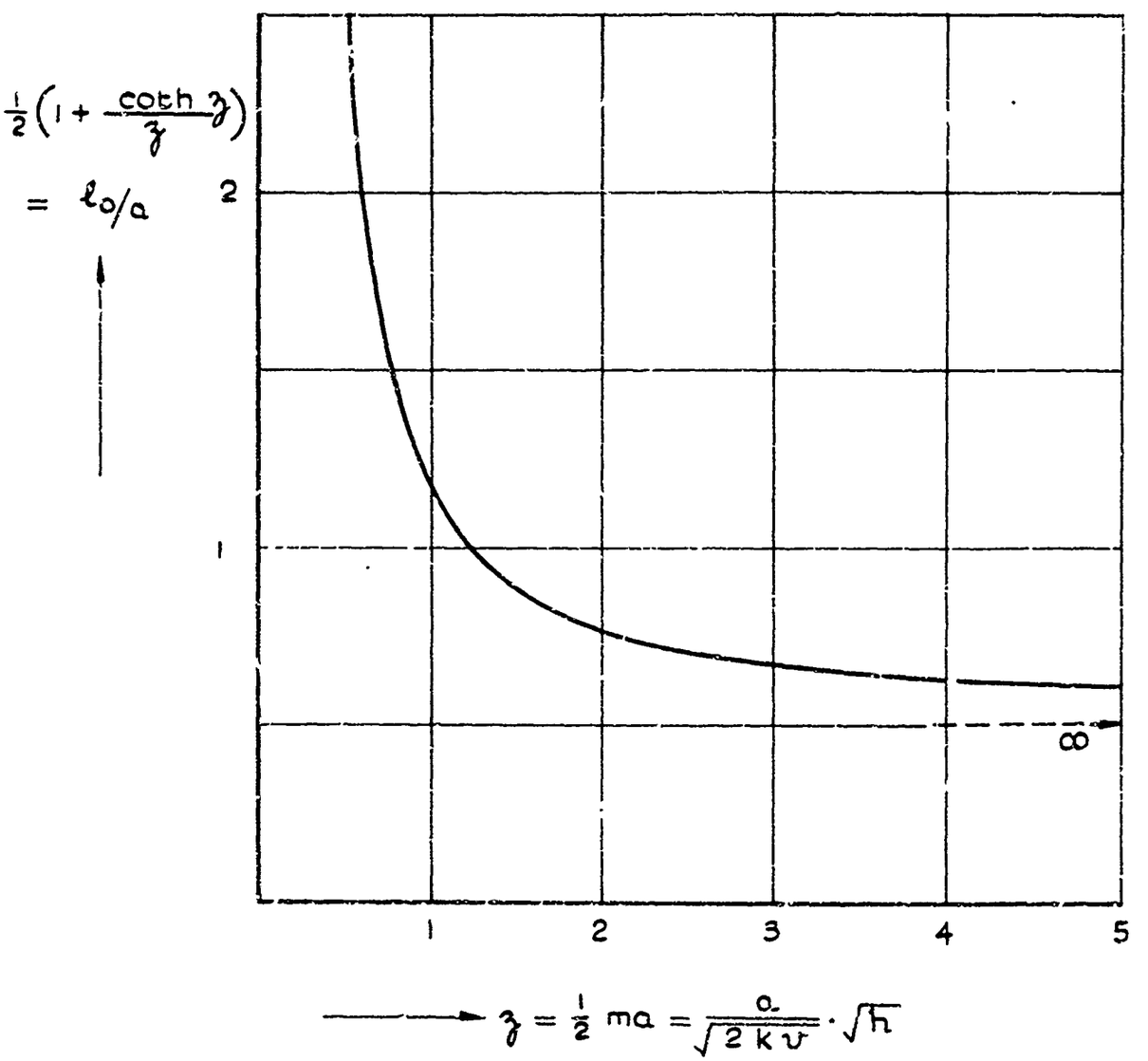

FIG. 8 $\frac{1}{2}\left(1+\frac{\coth \zeta}{\zeta}\right)$ VERSUS ζ